



School of Chemistry

Chemical Vapour Deposition of Diamond
under Static Flow Conditions

Matylda Chojak

**This thesis is submitted in partial fulfilment of the requirements for the Honours
Degree of Bsc Chemical Physics at the University of Bristol**

Supervisor: Neil Fox
Second Assessor: Paul May
Bristol University Diamond Group

April 2022

Abstract

Research is presented for the evaluation of CVD diamond growth under static flow conditions. Boron-doped diamond was deposited using Microwave Plasma CVD method and the effect of gas flow on its properties was investigated. The primary aim of this project was to optimise static mode growth parameters to produce diamond films of high quality and isotopic purity with high growth rates. The method involved the introduction of gases into the chamber in regular time intervals instead of flowing them continuously throughout the deposition. Varying the intervals allowed for an in-depth analysis of the as-grown material, which included OES acquisition of the plasma during deposition, and it was followed by Raman and SEM analysis of the resulting sample. Static flow approach, introduced for the first time in 2020 by Croot *et al.*, proved to increase the carbon efficiency during the process and therefore allowed for more economical production of diamond. The material waste was minimised by reducing the gas input during the reaction, which can be particularly advantageous when the feedstock gases used in the process are limited, expensive or hazardous to the environment. The experiment described in this body of work further explores the static mode approach and shows that the quality of the diamond grown under these conditions appears unchanged and various samples are of similar morphology. Furthermore, the results showed that static growth runs produce films of higher phase purity than films grown under continuous flow conditions; however, the static flow growth rates were significantly reduced due to insufficient levels of carbon radicals in the reaction chamber. Graphite etching was a crucial factor during deposition, and it was highly encouraged by the static mode growth, which contributed to overall quality of the as-grown material. Through Raman analysis it was shown that these films contained less graphitic components while their diamond centres remained almost unchanged. Future work is presented in the last part of the thesis.

Acknowledgements

Firstly, I would like to thank my project supervisor Neil Fox as without him this project wouldn't have been possible.

I would also like to thank Ed Smith for his endless help, patience and all his time spent supervising and teaching me the ways of the reactor and other analytical instruments.

Special thanks to Muj Abbas for being by my side throughout the whole experiment and for spending countless hours on getting our growth runs done.

Lastly, I would like to thank James Smith for his supervision in the lab and interest in the project, and the rest of the Diamond Group for making me feel welcome during my time in the lab and making this project a fun experience.

Contents

1	Introduction	1
1.1	Diamond and its properties	1
1.2	Synthesis of diamond.....	1
1.2.1	History.....	1
1.2.2	Chemical Vapour Deposition.....	2
1.3	CVD growth.....	3
1.3.1	Synthesis methods.....	3
1.3.2	Boron doping	5
1.3.3	Static flow growth.....	6
2	Experimental	7
2.1	Reactor schematic	7
2.2	Closed chamber growth	8
2.2.1	Substrate seeding.....	8
2.2.2	Operation of the reactor	8
2.2.3	Sample set	8
2.3	Characterisation techniques	9
2.3.1	Optical Emission Spectroscopy	9
2.3.2	Raman spectroscopy	10
2.3.3	Scanning Electron Microscopy	12
3	Deposition results and analysis	13
3.1	OES analysis	13
3.2	Raman analysis	15
3.3	SEM analysis	18
4	Future work	20
4.1	OES test	20
4.2	Use of isotopic diamond in radio voltaic batteries.....	20
4.3	Secondary ion mass spectrometry analysis.....	21
5	Conclusion	22
	References	23

1 Introduction

1.1 Diamond and its properties

Diamond exhibits a range of exceptional properties, making it a particularly desirable material for a great number of applications (Table 1). It is also an ideal crystal to study isotope effects, with a natural content of stable carbon isotopes consisting of 98.93% of ^{12}C and 1.07% of ^{13}C [1]. Carbon atoms are tetrahedrally bonded to each other with sp^3 hybrid bonds, however, a common polycrystalline diamond consists of randomly aligned diamond grains and rather weak grain boundaries, which contain sp^2 carbon [2]. Diamond has the highest atomic density, which results in a tight diamond lattice, making it difficult to substitute any element for carbon, as that would require large amounts of energy [3,4]. The extraordinary hardness of diamond makes it useful in the production of abrasive, shaping or cutting tools. Furthermore, its high thermal conductivity allows for thermal management of various electronic devices.

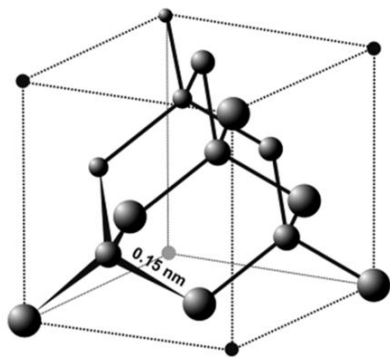


Figure 1 Body centred cubic structure of diamond [5].

Extreme mechanical hardness (100 GPa)
Highest thermal conductivity ($2 \times 10^3 \text{ W m}^{-1} \text{ K}^{-1}$)
Strongest material with the highest bulk modulus ($1.2 \times 10^{12} \text{ N m}^{-2}$)
High bandgap (5.47 eV)
High carrier mobility of electrons ($2400 \text{ cm}^2 \text{ V}^{-1} \text{ s}^{-1}$)

Table 1 Some of the unique properties of diamond [5].

1.2 Synthesis of diamond

1.2.1 History of diamond growth

The modern era of diamond growth began in the early 1950's. Diamond, with its wide range of exceptional properties, was a subject of intense research to scientists all over the world such as Eversole's research group in the US or Derjaguin's group from the Soviet Union [6]. The former successfully deposited diamond from carbon monoxide onto the diamond under metastable conditions in 1952. However, the deposition rates were low and production costs high [7]. In December 1954, scientists from General Electric laboratories managed to replicate the high pressure, high temperature (HPHT) conditions under which diamond naturally forms. It was the first method of diamond synthesis to be industrialised, but it had its limitations. Even though it was possible to grow single crystals of diamond, the grains were not of high quality, often containing metal inclusions, and their size was restricted. The HPHT method was also very expensive, given the energy and equipment required. Around the same time researchers investigated using Chemical Vapour Deposition (CVD) to grow diamond. Eversole and Deryagin et al. performed a homoepitaxial diamond growth by thermal decomposition under reduced pressure; however, the growth rates were still very low.

The breakthrough occurred in the 1960s, when Angus *et al.* introduced the presence of atomic hydrogen during deposition, which led to etching of graphite and formation of pure diamond. Subsequently, CVD diamond growth by heteroepitaxy was also investigated.

1.2.2 Chemical Vapour Deposition

The diamond synthesis method described in this body of work is Chemical Vapour Deposition (CVD), which is based on diamond growth in metastable regime. In the presence of suitable substrate, diamond films with large areas can be produced. The diamond CVD mechanism involves dissociation of precursor gases (CH_4 and H_2) into reactive species (H atoms and methyl radicals), which diffuse towards the surface of a solid material where they adsorb and coalesce to form a carbon film. Each CVD technique requires a mean of activating the gaseous reactants such as microwave radiation in MWCVD, hot filament in HFCVD or direct current in DC PACVD. Under suitable deposition conditions diamond films are formed [8]. Carbon is deposited mainly in the graphite form with a small amount of diamond, which is then followed by selective etching of graphite by hydrogen atoms [9]. CVD reaction also operates at temperatures greater than $700\text{ }^\circ\text{C}$ to ensure diamond formation rather than amorphous carbon.

As opposed to HPHT or natural diamond, CVD diamond can be deposited on shaped substrates, as well as on non-diamond substrates through heteroepitaxial growth [10]. CVD processes also operate at lower pressures and therefore can be performed using simpler and cheaper equipment. Diamond synthesis using CVD contributed to reduced costs of the material allowing to the extreme properties of diamond. Properties of CVD diamond include high radiation hardness, high time resolution and fast time response.

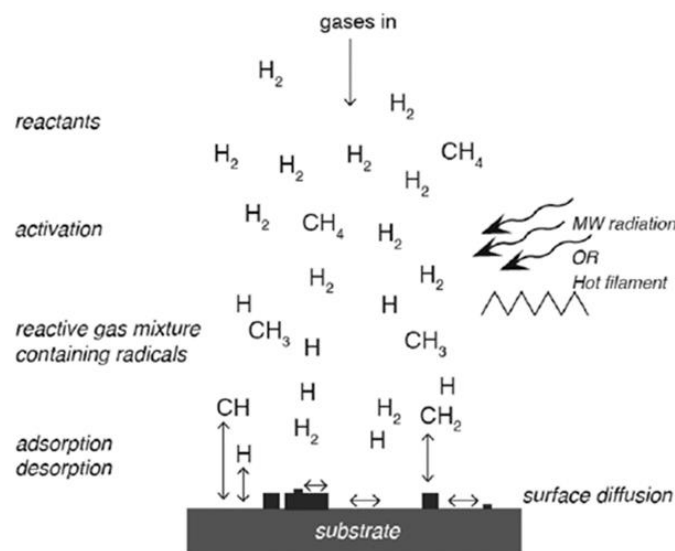


Figure 2 Schematic description of the CVD process [11].

1.3 CVD growth

1.3.1 Synthesis methods

The following section reviews the most common diamond CVD growth methods. All techniques utilize low pressures and the same sources of gaseous species involved in the deposition.

Hot filament CVD

Hot filament CVD (HFCVD) method is the earliest and most common method used for diamond growth due to the simplicity of the mechanism and comparatively low cost of the equipment, as well as being the most reproducible way to perform diamond growth at low pressures [12,13]. This deposition process was introduced by Matsumoto *et al.* in 1982 who studied heteroepitaxial nucleation of diamond under low-pressure CVD conditions [14]. It was also the first method to execute a continuous growth of diamond on various substrates.

The mechanism involves a tungsten filament, which is heated to a temperature above 2000 °C. CH₄ and H₂ gases pass through the filament, H₂ thermally dissociates into atomic hydrogen and CH₄ undergoes hydrocarbon pyrolysis to form methyl radicals. Dissociation of gas molecules enhances their reactivity and leads to diamond deposition on the adjacent substrate [15].

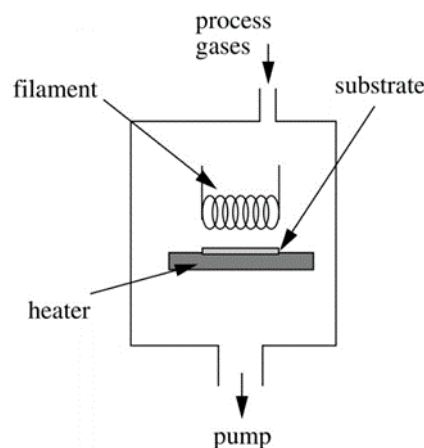


Figure 3 Schematic diagram of HFCVD reactor [16].

Produced polycrystalline films are of good quality with growth rates varying from 1 to 10 $\mu\text{m/h}$, depending on exact conditions during deposition process [16]. Deposition rate on the order of 1 $\mu\text{m/h}$ is typically associated with high-quality films [13]. HFCVD techniques also have its limitations. One of them is the stability of the filament, which can be affected by corrosion of the filament material during deposition, which limits the variety of gases that can be used in the process. High temperatures can also lead to metal evaporation from the filament, resulting in the incorporation of filament atoms into the grown film.

Direct Current plasma-assisted CVD

DC-PACVD method was first introduced by Suzuki *et al.* in 1987 [17] who suggested that diamond thin films could be formed at higher growth rates compared with other growth methods. The PDR (a pulsed-DC PA-CVD reactor) consists of two electrodes: a water-cooled cathode, usually made of Mo, Cu or Ta and the anode on which the substrate is placed during the growth. This particular CVD method requires specific deposition conditions within the reactor such as very high substrate temperatures, sometimes as high as 1300 °C [19]. High melting point substrate materials are therefore crucial for the growth process and so metals such as Mo, W or Ta are the usual choice. One of the outstanding features of the process is the excellent plasma stability and uniformity [19]. The gas phase chemistry is supplied by the energy from plasma discharge and heating through electron bombardment rather than by thermal energy coming from high process temperatures [18]. Energetic bombardment of the growing film is a result of an electrical bias, which helps to accelerate ions towards the substrate. The method is currently the most prominent and effective for synthesis of large single crystals of diamond, with the growth rates as high as 150 $\mu\text{m}/\text{h}$ [20].

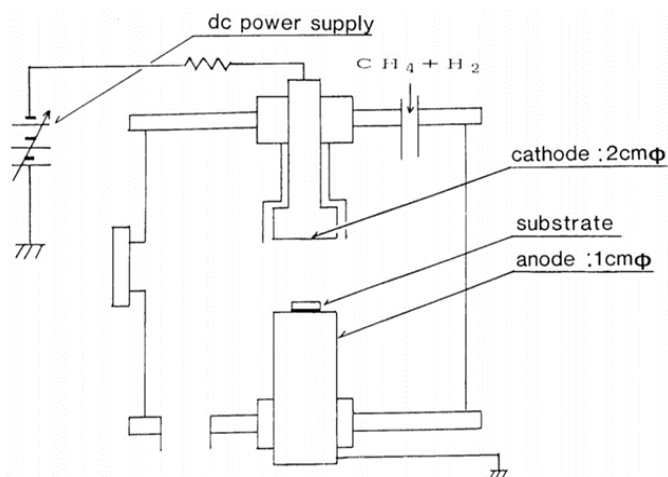


Figure 4 Typical DC PA-CVD reactor schematic [17].

Microwave Plasma CVD

The most widely used technique in diamond synthesis is Microwave Plasma CVD (MWCVD). It was first introduced by Kamo *et al.* in 1983, providing a way to obtain high-quality diamond film with minimal defects and high transparency [21]. MWCVD uses microwaves to ignite the plasma, which leads to the activation of the gas phase. This technique is highly reliable, efficient and provides cleaner environments for the film deposition than other CVD methods such as HFCVD; high temperature filaments generate significant amount of metal impurities, which are hard to mitigate [22] and lead to poorer quality of the film. Reported growth rates obtained during the process can be as high as 70–165 $\mu\text{m}/\text{h}$ [23]. This method also provides a scale-up capability for larger substrates [24]. MWCVD technique results in the formation of polycrystalline diamond, which yields various

electrical and optical properties, making it useful in a range of applications such as producing hard coatings, optical windows, or electrochemical electrodes [25,26].

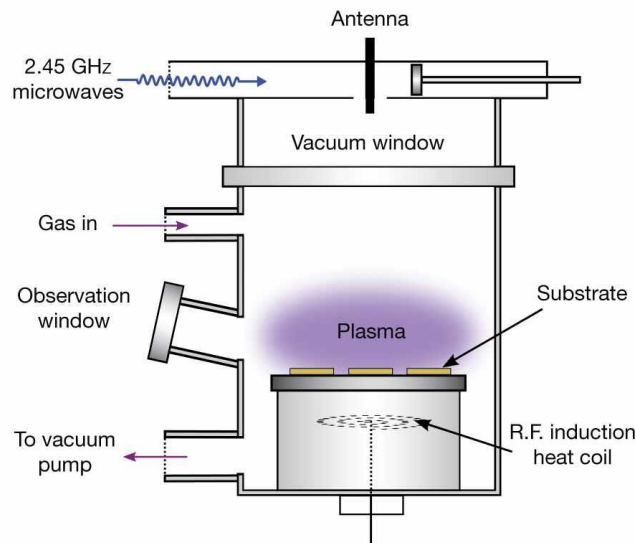


Figure 5 Schematic diagram of Microwave plasma CVD reactor. Microwave plasma acts as a mean of activating the gas phase [27].

1.3.2 Boron doping

Another factor investigated in this body of work is the role of dopants in the CVD diamond synthesis. Previous studies examined the influence of doping on growth rates, surface morphology and electrical properties of thin diamond films [28-30]. N, B, P and S are the most commonly investigated dopants due to their significant impact on the diamond properties and CVD growth mechanism. For this study, it was of interest to examine the role of diborane gas in the synthesis of boron-doped diamond.

Unlike Nitrogen [29], the presence of B in the gas phase only slightly affects the growth rate, though at high B concentrations the growth will decrease with increasing diborane levels. However, it was found that boron addition affects the surface morphology of the diamond and leads to an improvement in the structural quality of the thin film; with graphitic inclusions being reduced and point defects effectively eliminated during deposition [31,32].

Adding different concentrations of B species to the precursor gas mixture during CVD diamond synthesis has also proven to affect the electrical properties of the resulting film. At lower doping levels, B acts as an electron acceptor within the lattice giving the diamond p-type semiconducting characteristics, whereas high B doping results in a diamond film with electrical properties similar to those of metallic materials.

Boron-doped diamond is widely investigated in the fields of power electronics, electrochemical sensors and the industrial production of semiconductor materials [33,34]. It has many unique properties such as a wide solvent window, which makes it a great electrode material [35]; low capacitance and background; chemical and dimensional stability in harsh environments [36], which is important for designing photoelectric devices [37].

1.3.3 Static flow growth

There are variety of factors that can affect the nucleation of diamond during the CVD process. Some of the process parameters include gas composition, the temperature of the substrate, substrate biasing or the rate of the gas flow within the reactor [38].

Gas flow rate is of great importance as it is directly related to the gas transport in the reactor and over the years it has been proven that it can have a strong impact on the nucleation and growth rate of diamond [39]. However, the exact relationship is still not fully understood and many researchers investigating this topic report some conflicting results and conclusions [40].

Work by Celli *et al.* showed that changes in the gas flow rate have an impact on diamond crystal structure and surface morphology but the deposition rate was not really affected [41]. On the other hand, Chowdhury *et al.* studied the effect of gas flow rate on the diamond growth rate on carbon steel under thermal CVD conditions and showed that the thin film deposition rate increased with increased gas flow rate [40]. Similarly, paper published by Yu *et al.* in 1999, indicated that the increase in the gas flow rate enhanced diamond nucleation [42].

Gas flow rates can also contribute to changes in morphology of the deposited films; with microcrystalline diamond thin films obtained at relatively low rates (30 sccm to 300 sccm) and nanocrystalline films formed at higher flow rates (above 300 sccm) [38]. The latter can be associated with higher fluxes of carbon containing species towards the solid surface, favouring secondary nucleation. Gas flow rate can also influence parameters like spatial uniformity of the sample, grain orientation, film conductivity and Raman spectra.

In 2020, A. Croot *et al.* described a different approach that could improve diamond CVD mechanism: using static flow conditions (zero-total gas flow environment) for diamond deposition, as opposed to continuous flow used in the previous studies [43]. Static mode growth was utilised by limiting the gas input during deposition, while still maintain optimal deposition conditions, as well as by increasing the growth residence times. Variation of gas residence times can account for changes in surface morphology such as differences in dominant facets within the film [41].

Their research suggested that using the static mode results in increased atom efficiency and reduced leakage of the feedstock gases used in the process, which could be hazardous and toxic to the environment. Such gases are also limited and expensive and therefore using static-flow conditions would be beneficial to manufacturers. One of the examples would be utilisation of $^{13}\text{CH}_4$ and $^{14}\text{CH}_4$ for isotopically pure, single crystal diamond growth. Deposition under static mode would lead to a reduction in hazardous material volume, which is particularly important for future work, where radioactive gases could be used to produce radio voltaic batteries.

Comparison of the influence of static- and continuous-mode on the samples shows that there are more similarities than differences between them. However, the static-flow model shows a 30-fold improvement in the carbon efficiency in the source gas into diamond. This is a promising approach, which can be explored further by using different, more suitable reactors, with different process optimization. The study in this thesis investigates the effect of the static-flow mode conditions on the diamond growth using a boron-doped MWCVD reactor.

2 Experimental

2.1 Reactor schematic

The microwave reactor used for the experimental part of this work was a custom-made reactor, originally used for plasma diagnostics, given to Bristol University diamond group by Element Six Ltd. on a loan. The reactor has a cylindrical shape with a quartz window position above the area where plasma forms and deposition reaction occurs. Forced-air cooling from a fan above the window prevents it from overheating. Microwaves at 2.45 GHz enter the chamber through a waveguide and are transmitted by an antenna to resonate inside the reaction chamber. The plasma is centred on the anti-node of the standing wave. The base and walls of the reactor are water-cooled to prevent overheating. Input gases enter the chamber via two diametrically opposed inlets and gas flow is controlled using mass flow controllers (MFCs). The pumping speed of the gas is regulated by opening and closing the butterfly valve. Constant pressure was kept within the chamber with the maximum value of 300 Torr and the maximum microwave power of 1.8 kW. 10mmx10mmx0.5mm (100) silicon substrate, previously seeded with nanodiamond, rested on a tungsten disk (1.25 inch in diameter) and a spacer wire below the disk (4 mil in diameter). Base deposition conditions for the experiment were: total pressure, $p= 150$ Torr, total power, $P= 1.5$ kW and total flow $F= 300$ sccm. Within the total flow: $F(\text{H}_2) = 294$ sccm, $F(\text{B}_2\text{H}_6) = 6.3$ sccm and $F(\text{CH}_4) = 12.5$ sccm (4% of methane in hydrogen).

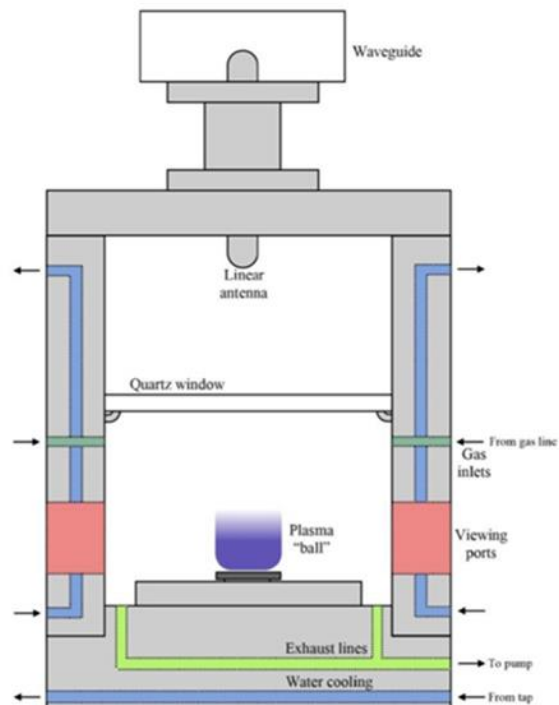


Figure 6 Schematic diagram of the boron doped MWCVD reactor chamber (University of Bristol) [44].

2.2 Closed chamber growth mechanism

2.2.1 Substrate seeding

Six silicon wafers (dimensions: 10mm x 10mm x 0.5mm) were seeded with nanodiamond using an electrospray method (NanoAmando® Aqueous Colloid Solution of detonation nanodiamond was used as a source). Seeding on non-diamond substrates enhances the growth rate by creating a homoepitaxial-like surface. The nanodiamond solution in methanol was first probed using ultrasonic pulses to break up the aggregates until a uniform solution was obtained. Silicon wafers were cleaned in an ultrasonic cleaning bath while submerged in methanol for three minutes. This was done to remove any residues remaining on the surface, from sources such as cutting processes, grease from hands or air in the lab. The samples were then dried using a compressed air gun. The seeding process involved accelerating the nanodiamond solution towards the Si plates by applying a potential difference ($P=60\text{kW}$) for over an hour. This provided a uniform coat of nanodiamond on the Si surface.

2.2.2 Operation of the reactor

Silicon substrates were placed on the tungsten disk in the chamber, which was then closed, aligned, and pumped down to few mTorr. The pneumatic valves were opened, and hydrogen gas was allowed into the chamber. Water-cooling was switched on as well as the blower (cooling fan) and the microwaves were enabled. Plasma was struck at 15 Torr with the striking power of 700 W. At this point the method changes depending on the chosen mode:

Continuous flow mode

The chamber pressure was increased to 150 Torr as well as the power, with the final value of 1.5 kW. Diborane and methane were introduced into the chamber at 50 Torr, causing plasma to change its colour from purple (pure hydrogen plasma) to green. The starting point of the run was marked once the chamber pressure reached 150 Torr. The gas flow was kept constant throughout the 2h run and the plasma intensity remained unchanged.

Static flow mode

Once the plasma formed, the pumping line was closed. At the same time diborane and methane gases were introduced into the chamber. Power and pressure were then steadily increased. At 150 Torr all gas valves were closed which marked the start point of the growth run. Gases were pumped into the chamber at specific intervals and changes in the plasma intensity were tracked using OES.

2.2.3 Sample set

In order to investigate the static flow growth, the following method was designed. Continuous flow CVD process requires a constant flow of gas throughout the whole run. Static flow approach minimises the amount of gas used during deposition by flowing the precursor gases into the chamber in regular intervals during the growth and sealing the reactor chamber in between each cycle so that only the species remaining in the chamber were involved in the growth. Varying the intervals at which the growth run was halted helped to investigate changes in the material growth over time.

The following cycles were chosen:

Growth Run	F120	ST120	ST60	ST40	ST30	ST20
Time interval at which the gases were introduced into the chamber (Minutes)	Constant throughout the run	0 (Beginning of the run only)	60	40	30	20

Table 2 Experimental shorthand and deposition times for closed chamber growth (ST) and continuous flow mode (F). In the case of ST120 sample, gases were introduced at the beginning of the run only. ST60 run represents the addition of the gases every 60 minutes throughout the run. Subsequently, the same method applied to the other static mode runs.

Each growth run was 2h long and at the beginning of each cycle (interval), gases were flowing into the chamber for one minute before the gas lines were closed. Standard 2h continuous flow growth run (F120) was also performed to provide a good comparison to the new static flow method.

2.3 Characterisation techniques

2.3.1. OES

Optical Emission Spectroscopy (OES) is a simple method used to perform plasma diagnostics during the diamond film deposition. It is used for probing species concentrations, atomic relative densities and temperatures of the gas and plasma discharge [24]. OES studies can be carried out on multiple gas chemistries to understand the behaviour of growth radicals in the plasma. Emission intensities are measured using a spectrometer coupled to a collection optic via a fiber optic cable pointed at the discharge inside the reaction chamber.

In 1993, Balstrino et al. performed the OES analysis on different plasma systems and found that the quality of the diamond film appears to be related to the ratio of the CH peak intensity to C₂ band intensity. He stated that the OES diagnostic method could be used as a way to optimise deposition conditions. However, for a given detection sensitivity, the OES only analyses a limited number of species that emit in the specific wavelength range [45].

The advantage of the OES method is the fast response to the plasma parameters in the reaction chamber [46]. The OES data is also useful in estimation of the power density of microwaves in the discharge as well as the etching rate of diamond in hydrogen plasmas.

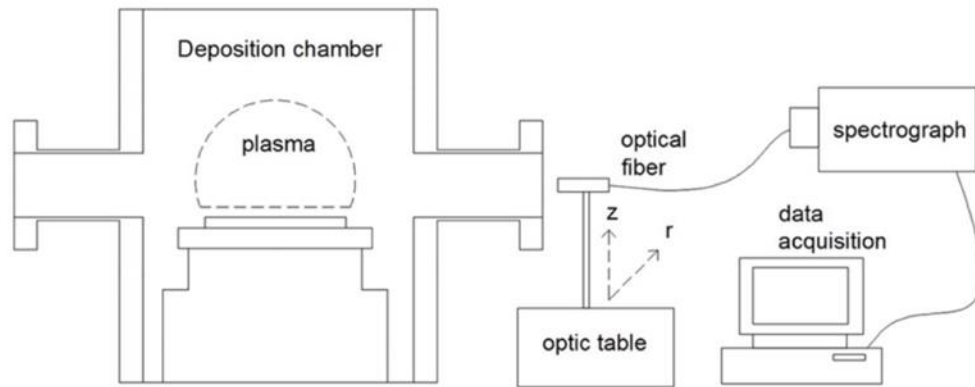


Figure 7 Optical emission spectroscopy setup used for plasma diagnostics during the CVD diamond growth [24].

The species of interest to be monitored by OES in this experiment are C_2 dimer emission at 516.52 nm, H_α emission at 656.81 nm and H_β emission at 486.31 nm.

Excited species	Electronic Transition	Peak position [nm]
CN	$B^2\Sigma^+ \rightarrow X^2\Sigma^+$	388.34
CH	$A^2\Delta \rightarrow X^2\Pi$	431.15
H_β	$n' = 4 \rightarrow n = 2$	486.31
C_2	$d^3\Pi_g \rightarrow a^3\Pi_u$	516.52
H_2	$3p^3\Sigma_u \rightarrow 2s^3\Sigma_g$	602.16
H_α	$n' = 3 \rightarrow n = 2$	656.81

Table 3 OES characteristics for the CH_4/H_2 plasma [24].

2.3.2 Raman spectroscopy

Raman spectroscopy provides qualitative characterisation of CVD diamond films and helps to find optimal growth process parameters. Different molecules have their own fingerprints and therefore different Raman spectra. This sensitive technique allows for identification of the variety of crystalline and disordered structures of a CVD diamond film [47]. It is possible to identify different hybridization states of carbon such as sp^2 (amorphous phase) or sp^3 , which corresponds to diamond. The mechanism is based on the Raman effect – the electron is excited to higher energy level due to photons and comes back with gain or loss of some energy. Photons may cause a change in polarizability of the molecule with respect to its vibrational motion, which induces a dipole moment. The number of excitations and emissions is provided using a high intensity laser light (diode excitation laser at 514nm was used as a light source in this thesis). Different forms of carbon exhibit different Raman shifts (Table 4).

Raman shift [cm^{-1}]	Interpretation
1580	Monocrystalline graphite
1546	Disordered graphite
1500-1600	Amorphous carbon sp^2 (G-band)
1430-1470	Trans-polyacetylene laying in the grain boundaries
1345	Amorphous carbon sp^2 (D-band)
1332	Diamond band
1220	Disordered diamond
12250, 1237	Nanodiamond
1100-1150	Trans-polyacetylene segments at the grain boundaries

Table 4 Raman shifts corresponding to different forms of carbon [47].

Raman analysis can also be used to measure the quality of the diamond. Different carbon forms (Figure 8) that grow on the substrate produce their own signals in the spectrum and therefore their peak intensities can be compared to the peak intensity of diamond. Analysing these ratios gives information about quality of the sample and allows for comparison with other films.

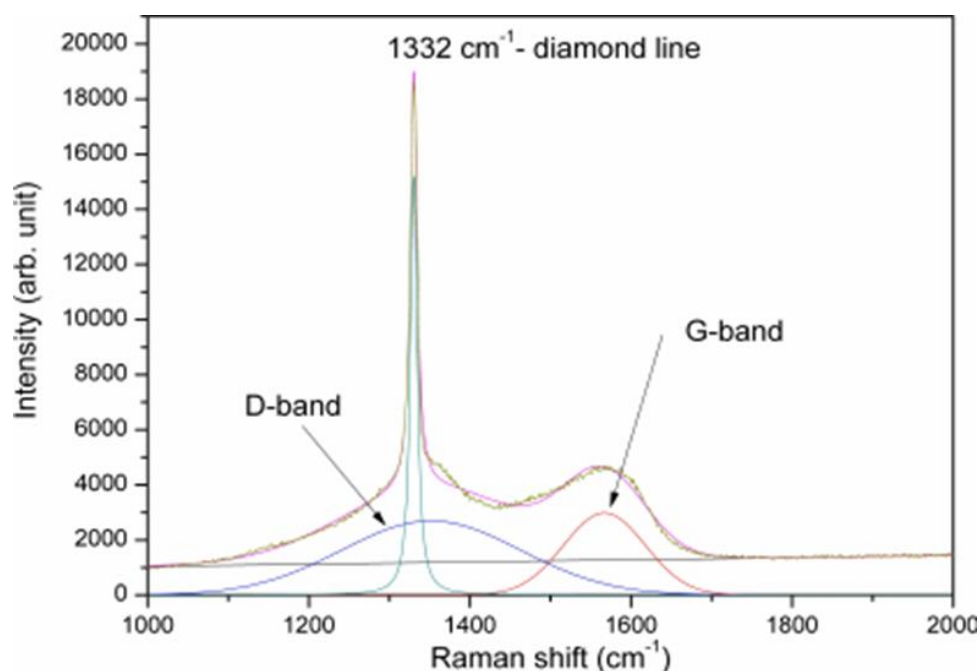


Figure 8 Raman spectra of diamond and two amorphous carbon phases [47].

Finally, another quality measure that can be obtained from the Raman spectra is full width at half maximum (FWHM), which gives information about the structural distribution. It is given by the distance between two points on the curve at which the function reaches half of its maximum intensity. The broadening of the peak indicates a degree of polycrystallinity in the

sample structure. For the same molecule, crystalline material will show a sharper peak than its amorphous form.

Raman spectrum with a single, narrow peak at 1332 cm^{-1} corresponds to high quality, single crystal diamond. As the change in FWHM is associated with changes in crystallinity of the diamond, large single crystals will exhibit small FWHM, while the smaller crystals will exhibit broader FWHM. This is due to dislocations and grain boundaries, which increase the strain in the crystal. A narrower peak is therefore indicative of diamond with better quality. FWHM values for single crystal diamond can be in a range as low as $3.3\text{-}3.5\text{ cm}^{-1}$ [48,49].

2.3.3 Scanning Electron Microscopy (SEM)

SEM is a mostly non-destructive method that produces detailed and magnified images of an object on the micro- to nanoscale. Electron microscopy has 1000 times better resolution than traditional light microscopy, making it useful for imaging biological specimens but also non-biological specimens such as crystals. Beams of electrons are projected and accelerated towards the specimen, which then scans the surface causing secondary electron discharge via inelastic collisions. Electron signal is then converted into a light signal and detected to produce a high-quality image.

High-energy electrons allow for a greater magnification than regular optical microscope. This is particularly useful when assessing the size and quality of diamond growth as well as measuring the thickness of the film, which provides a way of calculating the growth rates.

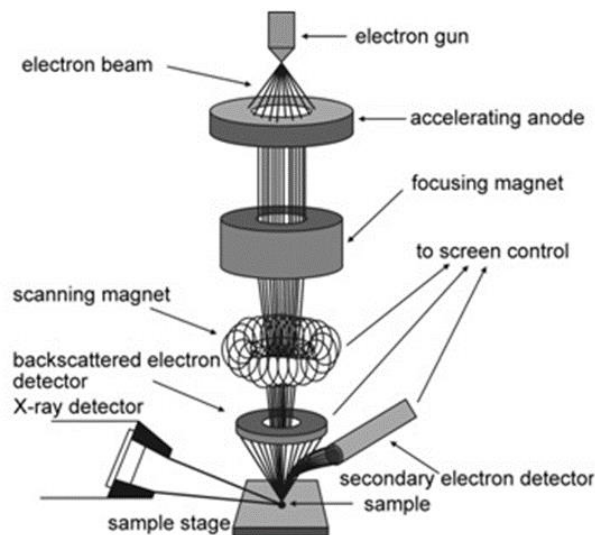


Figure 9 Scanning Electron Microscopy (SEM) setup [50].

3 Deposition results and analysis

The following section evaluates the diamond growth under static flow using MWCVD by providing comparative values for literature work and an in-depth analysis of the process using characterisation techniques. Different analytic methods increase the understanding of the deposition process by investigating the structure, surface morphology and quality of grown diamond films as well as the growth itself, through analysis of plasma chemistry at different points during deposition.

3.1 OES analysis

Broadcom® Qmini OES spectrometer was used to monitor emission intensities of growth radicals during each deposition run. The system was set to collect spectra every 300s for 130 min and the wavelength coverage was set from 200nm to 1000nm.

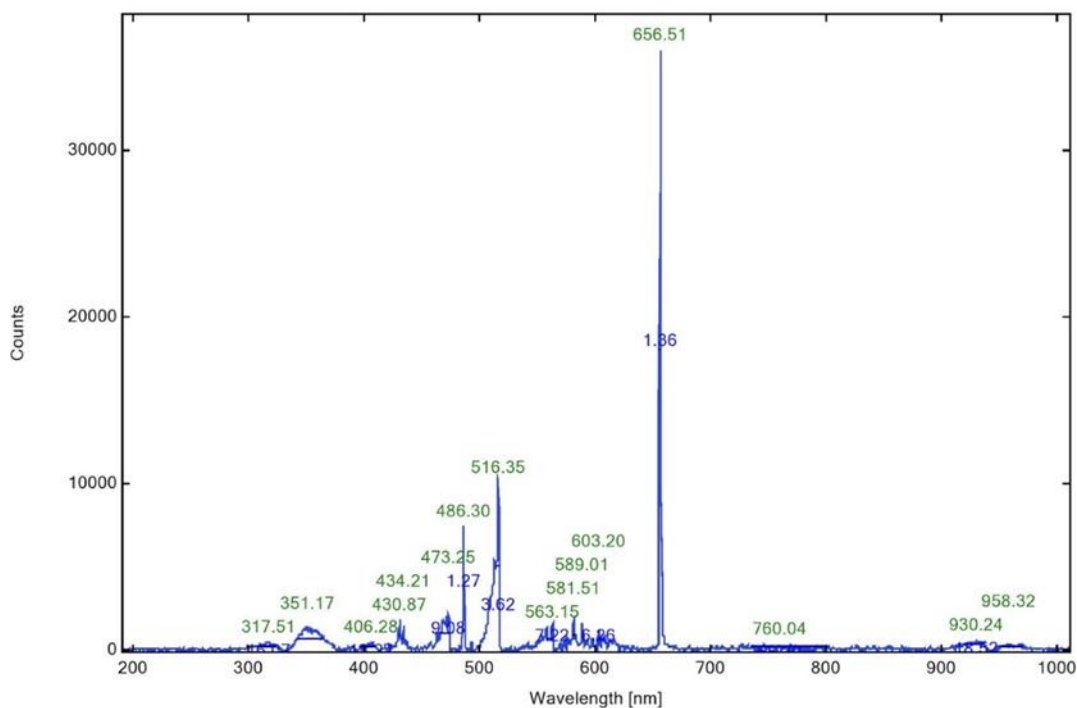


Figure 10 Reference OES spectrum. Following species can be identified from the spectrum: C_2 dimer emission at 516.35 nm, H_α emission at 656.51 nm and H_β emission at 486.30 nm.

Static mode analysis

The experimental work was done on six samples, five of which investigated the static flow mode and the last one investigating the continuous flow. The following graph represents the OES analysis of normalised emission intensity of C_2 dimer during a 120 min run, showing the repeated static flow cycles and points at which the gas chemistry in the reactor chamber returns to its initial conditions. An increase in the intensity corresponds to the addition of methane into the chamber and therefore an increase in the methyl radicals in the plasma. As the reaction proceeds and more diamond is deposited on the substrate surface, the amount of C_2^* species decreases, and the plasma emission is dominated by the hydrogen Balmer series. This can be easily observed as the plasma ball becomes more purple with time.

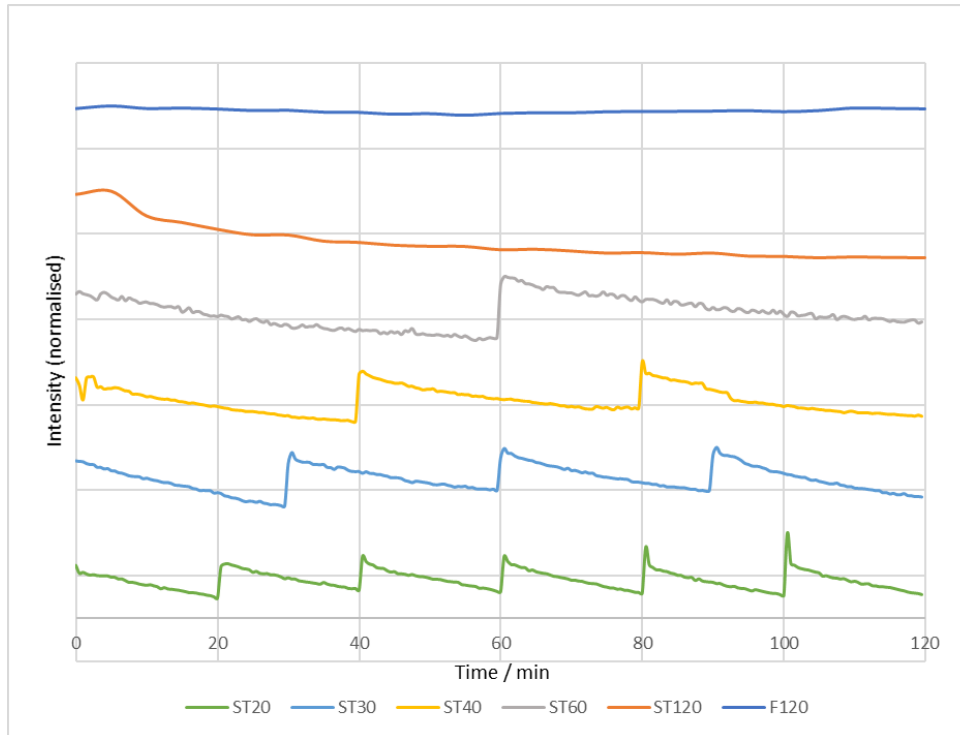


Figure 11 Graph of normalised emission intensity of C_2 dimer during a 2h run. Datasets have been vertically offset for clarity.

The F120 plot corresponds to a 120 min continuous gas flow run. As all the gases are continually introduced into the chamber, the C_2 intensity remains constant. Consistent supply of methane creates a good environment for diamond growth; however, the quality of the resulting film cannot be evaluated using OES and therefore other analysis techniques need to be performed.

The ST120 plot corresponds to a 120 min static flow run, where the only introduction of gases occurs at the start of the reaction. As the reaction proceeds, methane is getting used up steadily and in the end of the deposition, the plasma emission shows drastically reduced emission from carbon-containing species.

The other four plots represent the intervals at which methane was allowed back into the chamber (for a specific amount of time, in this case one minute) and therefore the C_2 emission intensity returned to the initial value. The plot lines are not smooth due to fluctuations in the pressure during deposition, but this specific trend can still be observed.

Decay constant

The emission intensities of C_2^* decay exponentially with time during static flow mode. The OES analysis allowed for calculation of decay constants for each growth run. The resulting values appear relatively similar, which indicates consistency in the method and therefore allows for further accurate comparison of the results. Calculations were performed using the following equation:

$$I(t) = I_0 e^{-\lambda t}$$

Where $I(t)$ is the emission intensity of C_2^* as a function of time, I_0 is the initial emission intensity of C_2^* and λ is the decay constant. The emission intensity of C_2^* during continuous

flow growth (F120) remains constant throughout the process and therefore the decay constant is approximately equal to zero.

Run	Decay constant / λ
ST20	0.04
ST30	0.03
ST40	0.03
ST60	0.02
ST120	0.03
F120	0.001

Table 5 Values of decay constants for different growth runs corresponding to exponential decay of C_2^* during deposition.

3.2 Raman analysis

Raman spectroscopy was used to confirm the presence and evaluate the quality of the diamond grown under various gas flow conditions. For the analysis of the results, a Renishaw 1000 system with a 1200 lines/mm grating was used and a green laser at 514 nm excitation wavelength was the main source of light. Leica® DM LM microscope with a 50x/0.75 N PLAN lens was used to view the samples, while a computer was used for data acquisition and curve fitting.

Reference plot

A dominant sp^3 diamond peak at 1332 cm^{-1} is characteristic of polycrystalline diamond as well as the contribution of sp^2 carbon (D-band, G-band) coming from the grain boundaries.

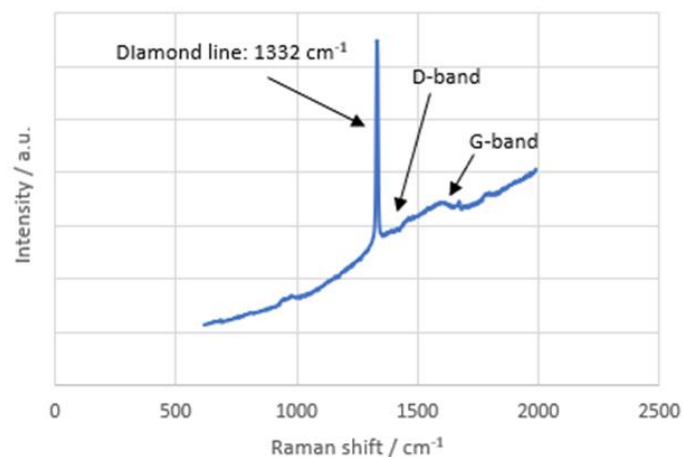


Figure 12 An example Raman spectrum showing groups of absorbance bands relating to composition of diamond surfaces.

Spectra analysis

Analysis of each spectrum was conducted with emphasis on identification of specific Raman peaks, comparison of HFHM values and description of observed trends corresponding to various flow modes.

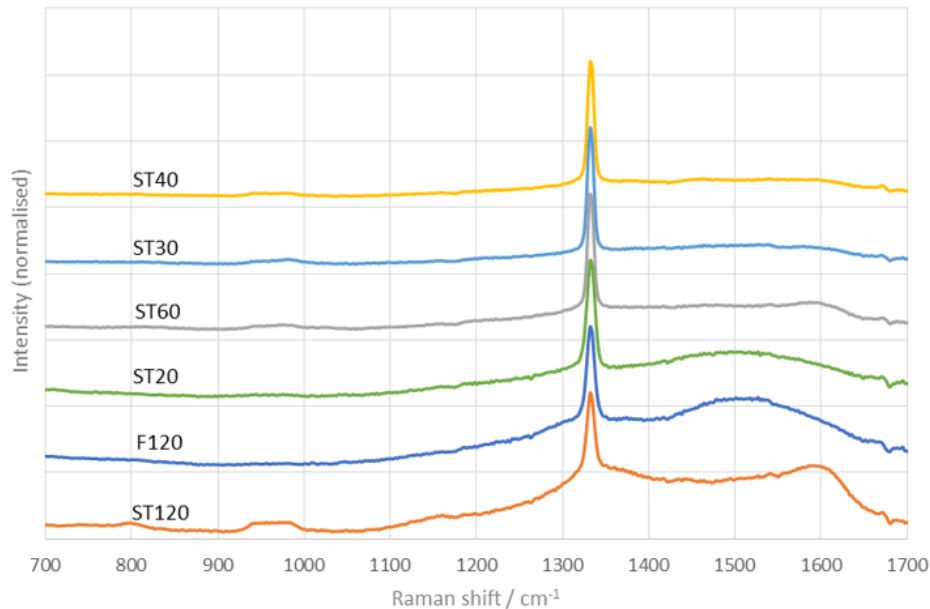


Figure 13 Raman spectra of a diamond nucleation on six samples obtained from a 2h run, presented with corresponding intensities normalised to the height of the 1332 cm^{-1} (vertical offset used to compare the spectra).

Etching

A significant factor affecting the diamond deposition is graphite etching by the hydrogen plasma. Diamond and graphite are both etched by atomic hydrogen; however, the CVD diamond growth rate outruns its etching rate. This does not apply to other carbon states such as graphite and therefore it is easier to etch it from the substrate surface. Static flow mode encourages etching when the gases stop flowing. The more hydrogen content relative to that of methane, the more time for sp^2 carbon to be etched. The aim of the static flow method is to maximise the graphite etching by extending the gas flow intervals while still providing enough methane for successful nucleation of diamond.

Trends

Figure 14 presents the Raman spectra of diamond nucleation on six CVD diamond films grown under static mode. Each spectrum presents different characteristics corresponding to various species environments within the material.

Silicon peak at 950 cm^{-1} was identified in the ST120 spectrum. Raman signal originates from a volume defined by the penetration depth of the laser and how far it penetrates depends upon its wavelength [49]. The observed trend implies a very thin diamond film and that is later confirmed by the SEM analysis. The sp^3 diamond peak was identified at 1332.44 cm^{-1} , while a significant raise in the intensity between 1400 cm^{-1} and 1600 cm^{-1} corresponded to a range of sp^2 environments formed within the film. The large sp^2 contribution results from surface damage caused by hydrogen bombardment, originating from low concentration of methane in the plasma. As all the gases are introduced only at the

beginning of the run, C₂ drops over time, and high concentration of hydrogen induces large amounts of etching. Repeated renucleation could also contribute to the observed trend.

F120 spectrum represents the constant flow of gases. The prominent graphitic peak at 1500 cm⁻¹ can be explained by a continuous supply of methane which encourages *sp*² nucleation. This in turn minimises the etching rate. The diamond centre was identified at 1332.34 cm⁻¹, with the value being closest to the literature (Table 4).

ST20 spectrum presents a graphitic “hump” around 1500 cm⁻¹, however, this is much broader and less prominent when compared to F120 spectra, which is a result of an increasing etching rate induced by static flow process. Relatively large amount of methane, due to the frequency of the cycles, encourages *sp*² nucleation. ST60 spectrum shows a significant reduction in the graphite peak (G-band) but it can still be observed. This might be explained by possibly too much etching due to a longer residence time (60-minute interval). Both ST20 and ST60 present a diamond centre at 1332.64 cm⁻¹ and 1332.63 cm⁻¹, respectively.

ST40 and ST30 spectra show the best results, with a sharp diamond peak at 1332.74 cm⁻¹ and 1332.43 cm⁻¹ respectively, as well as with the graphitic peak being significantly reduced. This represents a good balance between the amount of methane present in the plasma and the etching rate. It can be concluded that the chosen intervals appear to provide the optimal conditions for static flow growth.

Comparing the diamond centres of each sample leads to a conclusion that diamond quality seems to not be affected by the static mode conditions, which is a result similar to that of Croot et al. [43] (this is also supported by the analysis of the FWHM of *sp*³ peaks for each sample, described below).

Full Width at Half Maximum (FWHM)

For the spectra containing diamond peaks, the FWHM of each peak was found. Narrower peaks suggest a structure closer to that of a natural diamond, which exhibits a FWHM of around 1.9 cm⁻¹ [51]. The results indicate that the ST60 growth run produced a diamond film with the narrowest FWHM, suggesting the best phase purity out of all the samples. Interestingly, the sample grown under continuous flow conditions exhibits the widest FWHM and therefore indicates a higher level of graphitic inclusions present within the film. This suggests that diamond growth under static mode conditions can lead to an improved phase purity, with a potential to grow single-crystal films while reducing the feedstock gas intake and material wastage during the process.

Run	Full Width at Half Maximum (FWHM) / cm ⁻¹
ST20	10.9
ST30	8.46
ST40	8.49
ST60	8.30
ST120	12.2
F120	12.9

Table 6 FWHM values of diamond peaks for each sample.

3.2 SEM analysis

SEM analysis was used to investigate the effect of gas flow on the surface morphology and the growth rate of diamond films. Images of six samples were collected using a high vacuum SEM and the thickness of each film was determined. By calculating an average thickness and dividing it by the growth time, it was possible to determine the growth rate for each sample. The averaging process involved measuring the cross-sectional thickness of the film at three different points on the sample to improve the accuracy of the measurement and provide a better estimate for the actual value.

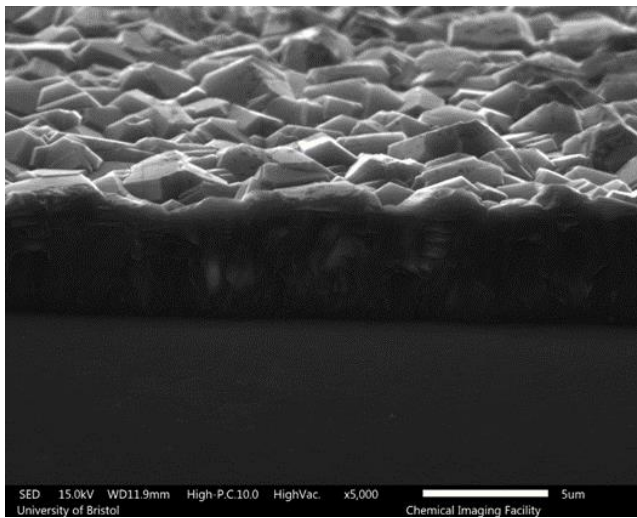


Figure 14 SEM image of cross section from middle of the cleaved edge (ST30 sample).

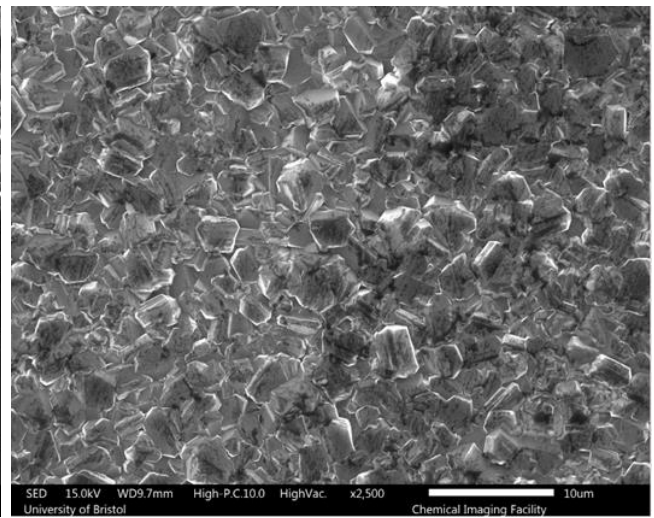


Figure 15 SEM top image at roughly the middle point of the ST30 sample.

The surface of the film grown under continuous flow conditions was the only one to contain the square {100} facets (Figure 16), as well as presenting the best thickness uniformity. However, the grains were not of a uniform size and multiple defects were observed across the surface. ST120 film contained the smallest grains and was significantly thinner when compared to other samples. This could be explained by considering a high level of etching present during deposition, resulting in substantial damage to the surface. ST20 and F120 runs produced the largest grains due to highest concentrations of methane present in the chamber during deposition (Table 7).

Sample	Grain width range (μm)
ST120	0.6-0.8
ST60	1.2-2.4
ST40	1.3-2.8
ST30	1.6-2.9
ST20	2.6-3.7
F120	2.8-3.8

Table 7 Grain width range for each diamond film sample (in μm).

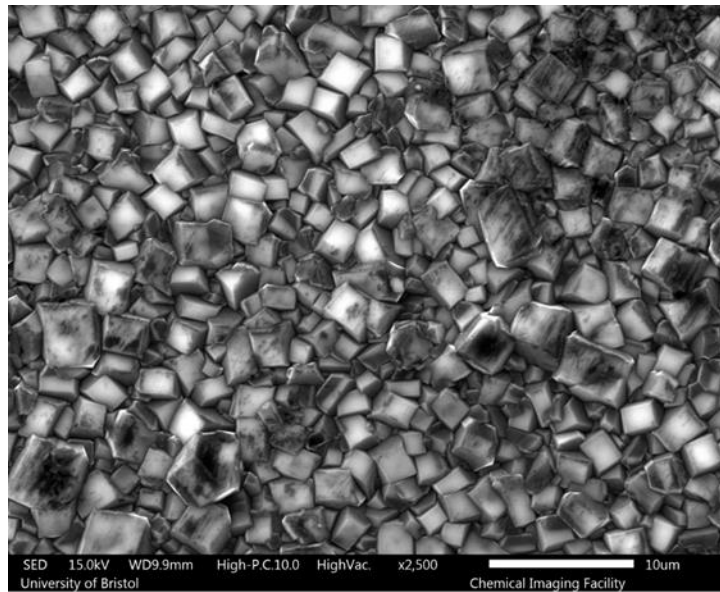


Figure 16 SEM image of F120 sample showing the presence of {100} facets within its surface.

Growth rates

Diamond film grown under continuous flow mode (F120) exhibited the greatest growth rate as a result of a constant supply of gases throughout deposition. The exact opposite can be said about the ST120 film, where the insufficient levels of CH radicals during growth had a direct impact on the surface morphology of the film, resulting in the thinnest layer of diamond after a 2h run.

Run	Growth rate / $\mu\text{m h}^{-1}$
ST120	0.32
ST60	1.13
ST40	1.84
ST30	2.47
ST20	3.93
F120	5.19

Table 8 Growth rates of six diamond films grown under varying gas flow, showing a general increase as the gases are introduced in shorter intervals.

As mentioned earlier, this is a trend supported by literature. Chowdhury *et al.* studied the effect of the gas flow rate on the diamond growth rate and proved that the thin film deposition rate will increase with increased gas flow rate [40].

4 Future work

4.1 OES test

An additional test was conducted in order to further explore the role of C_2 in the diamond growth process using OES analysis. The system was recalibrated with the trigger interval of 0.25s for 2 min. The test evaluated the point during the run at which gases are reintroduced into the reactor chamber. The aim was to measure how long it takes for the C_2 peak to hit its maximum intensity and to stabilise, which is equivalent to the optimal amount of methane that is present in the chamber at the initial deposition conditions.

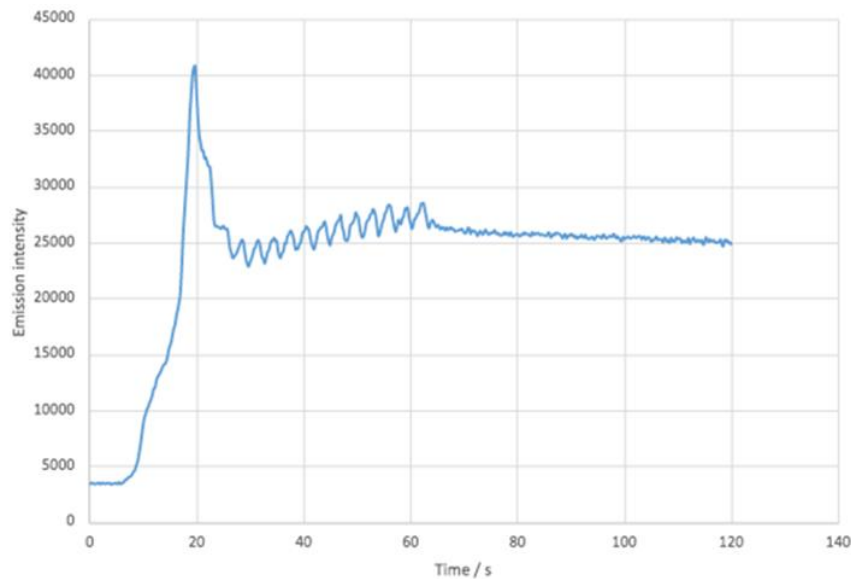


Figure 17 OES test to determine the gas flow time required to reach initial methane concentration.

The results show that it takes about 30 seconds for C_2 to reach its maximum emission intensity and stabilise, which means that during the static flow run, 30s is enough time to reintroduce the gases and reach the initial methane concentration. While in this body work, the gas flow was allowed for one minute, this additional test provides a significant improvement to the experiment, leading to reduction of material waste and contributing towards more economical production of diamond during long growth cycles.

4.2 Radio voltaic batteries

Since the early 1900s, researchers have been trying to find a way to turn radioactive material into an electric current source. The solution was a nuclear battery, which was made by Henry Moseley in 1913 [52]. This type of battery was of great interest due to the long-life power supply, high energy density, minimal external maintenance, and environmental adaptability [53]. Furthermore, nuclear batteries have a wide range of applications in military and biomedical fields as well as in aerospace, underwater or wireless communication systems [54].

In 1954, Rappaport et al. published their work on the photovoltaic effect [55] and around the same time the first beta particle induced electron-voltaic effect was reported [56]. Since then,

a new type of nuclear battery has been studied called a radio-voltaic (RV) cell; much smaller than the radio-thermoelectric generator (RTG) which was a main type of nuclear battery used within the field at the time. RV cells were particularly useful for small electronic devices such as sensors, implanted medical devices or microchips. Two types of RV cells are alpha-voltaic (AV) and beta-voltaic (BV) cells.

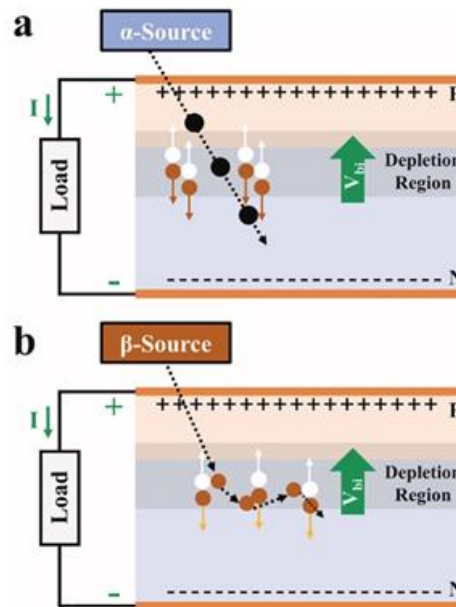


Figure 18 Operation mechanism for RV cell: (a) AV cell and (b) BV cell [53].

Recently, RV cells based on diamond diodes have been investigated [57]. Diamond is a wide-band gap semiconductor with high radiation resistance and batteries based on the photovoltaic effect and made of diamond show an improvement in total conversion efficiency. Most diamond nuclear batteries use boron-doped diamond in their structure – boron gives the diamond the p-type semiconducting characteristics.

Alpha-sources contain higher energy than beta-sources, as well as having a longer half-life and lower self-absorption energy. This means that AV cells can potentially increase the power density and power conversion efficiency of the RV nuclear cells.

However, the development of AV cells still has its limitations: there is a significant amount of radiation damage to the diamond, which leads to degradation of the cell performance and the levels of power conversion efficiency are usually low. There is also a contradiction between power density and stability [53].

4.3 Secondary Ion Mass Spectrometry analysis

Work described in this paper investigates the CVD growth of boron-doped diamond. Gas-phase boron was incorporated into bulk diamond, affecting its semiconducting characteristics. SIMS analysis is another method used in structural and compositional characterisation of CVD films and is commonly used to obtain depth profiles of dopants [58]. It analyses the depth distribution of the concentration of boron and allows for identification of the broadening effects within the sample and measurement of B-doping efficiency. Heavily boron-doped Si layers are a preferable material for the study of depth resolution in SIMS. Therefore, samples presented in this research can provide valuable information on the effect of boron on the structure of diamond grown under static flow conditions [59].

5 Conclusion

The primary aim of this research was to explore the growth of zero total flow within a MWCVD, assessing the variation in the OES spectra and the boron-doped diamond grown. Different characterisation methods were used to analyse the surface morphology and phase purity of diamond films, as well as the growth rates and the effect of the gas flow on the quality of grown material.

Initially, specific intervals at which various growth runs were halted, were carefully chosen, with the aim to find optimal conditions, which would result in production of the diamond film with the best quality and the highest growth rate. After producing and analysing the six diamond film samples, it was possible to observe different trends in the Raman spectra and SEM images corresponding to chosen intervals/ modes in each deposition run.

By comparing the FWHM values for each film, the results showed that the diamond quality remained unchanged during different growth runs. This suggests that the conditions used were approaching the optimal growth conditions. However, FWHM values for static growth were significantly lower than the one corresponding to continuous flow, suggesting that diamond growth under static mode conditions can lead to improved phase purity, with a potential to grow single-crystal films.

Introducing the gases at specific intervals, as opposed to continuously flowing them into the chamber, also had an effect on the graphite etching rates, with longer intervals leading to reduction in graphitic inclusions within the film.

Through SEM analysis, it was found that the growth rates were maximised during continuous flow and were decreasing under static mode as the intervals became longer. A higher concentration of methane within the chamber led to an increase in the nucleation rate, however, this encouraged the formation of sp^2 carbon on the substrate surface due to lower etching rates. ST40 sample appeared to provide the best deposition conditions, with a good balance between the etching rate and the amount of methane in the chamber, which allowed for successful deposition of diamond. The reduction in the graphitic component within the films could also be explained by the presence of diborane gas during deposition, as boron doping helps to improve the structural quality of diamond films. Furthermore, the ST20 and F120 produced the largest grains as a result of higher concentration of methane present in the chamber during deposition.

Overall, limiting the gas input during static flow deposition is a promising way of maximising the carbon efficiency and reducing the material waste. This is a big improvement to the continuous flow deposition method, especially when considering the use of expensive, rare, or hazardous precursor gases. Static flow mode can be applied to different CVD methods and hopefully lead to deposition of isotopically pure, single crystal diamond films.

References

- [1] M. N. Magomedov, "The baric properties of isotope-pure diamonds from ^{12}C and ^{13}C ," *Materials Today: Proceedings*, vol. 5, pp. 26025-26032, 2018
- [2] Q. Liang, C.-S. Yan, Y. Meng, J. Lai, S. Krasnicki, H.-K. Mao, R. J. Hemley, "Recent advances in high-growth rate single-crystal CVD diamond," *Diamond and Related Materials*, vol. 18, pp. 698-703, 2009
- [3] W. F. Banholzer, T. R. Anthony, "Diamond properties as a function of isotopic composition," *Thin Solid Films*, vol. 212, pp. 1-10, 1992
- [4] W. F. Banholzer, T. R. Anthony, "Properties of diamond with varying isotopic composition," *Diamond and Related Materials*, vol. 1, pp. 717-726, 1992
- [5] J. J. Gracio, Q. H. Fan, J. C. Madaleno, "Diamond growth by chemical vapour deposition," *Journal of Physics D: Applied Physics*, vol. 43, p. 374017, 2010
- [6] R.C. DeVries, A. Badzian, R. Roy, "Diamond Synthesis: The Russian Connection," *MRS Bulletin*, vol. 21, pp. 65-75, 1996
- [7] L. L. Regel, W. R. Wilcox, "Diamond film deposition by chemical vapor transport," *Acta Astronautica*, vol. 48, pp. 129-144, 2001
- [8] M. Ashfold, P. May, C. A. Rego, N. M. Everitt, "Thin Film Diamond by Chemical Vapour Deposition Methods," *Chemical Society Reviews*, 1994
- [9] J. Gracio, Q. Fan, J. Mendes, "Diamond growth by chemical vapour deposition," *Journal of Physics D: Applied Physics*, vol. 43, p. 374017, 2010
- [10] R S Balmer, J R Brandon, S L Clewes, H K Dhillon, J M Dodson, I Friel, P N Inglis, T D Madgwick, M L Markham, T P Mollart, "Chemical vapour deposition synthetic diamond: materials, technology and applications," *Journal of Physics: Condensed Matter*, vol. 21, p. 364221, 2009
- [11] A. Bogaerts, M. Eckert, M. Mao, E. Neyts, ,, Computer modelling of the plasma chemistry and plasma-based growth mechanisms for nanostructured materials," *Journal of Physics D: Applied Physics*, vol. 44, p. 174030, 2011
- [12] A. Mallik, "Hot Filament CVD Growth of Polycrystalline Diamond Films and its Characterisation," 2003
- [13] H. Liu, D. S. Dandy, "3 - Diamond CVD Techniques," *Diamond Chemical Vapor Deposition*, pp. 14-45, 1995
- [14] R Haubner, B Lux, "Diamond growth by hot-filament chemical vapor deposition: state of the art," *Diamond and Related Materials*, vol. 2, pp. 1277-1294, 1993
- [15] D. Cameron, "Optical and Electronic Properties of Carbon Nitride," *Surface & Coatings Technology*, vol. 169, pp. 245-250, 2003

- [16] P. W. May, "Diamond thin films: a 21st-century material," *Philosophical Transactions of the Royal Society A*, vol. 358, pp. 473-495, 2000
- [17] Atsuhito Sawabe, Hiroaki Yasuda, Tadao Inuzuka, Kazuhiro Suzuki, "Growth of diamond thin films in a DC discharge plasma," *Applied Surface Science*, vol. 33-34, pp. 539-545, 1988
- [18] D. Lundin, H. Pedersen, "High Power Pulsed Plasma Enhanced Chemical Vapor Deposition: A Brief Overview of General Concepts and Early Results," *Physics Procedia*, vol. 46, pp. 3-11, 2013
- [19] Ki-Woong Chae, Young-Joon Baik, Jong-Keuk Park, Wook-Seong Lee, "The 8-inch free-standing CVD diamond wafer fabricated by DC-PACVD," *Diamond and Related Materials*, vol. 19, pp. 1168-1171, 2010
- [20] S.A. Linnik, S.P. Zenkin, A.V. Gaydaychuk, A.S. Mitulinsky, "High-rate growth of single crystal diamond in AC glow discharge plasma," *Diamond and Related Materials*, vol. 120, p. 108681, 2021
- [21] Sun Q., Wang J., "Study on the Large Area Diamond Film Deposition in a Self- built Overmoded Microwave Power Chemical Vapor Deposition Device," *Chemical Engineering Transactions*, vol. 62, pp. 1129-1134, 2017
- [22] J. Weng, F. Liu, L.W. Xiong, J.H. Wang, Q. Sun, "Deposition of large area uniform diamond films by microwave plasma CVD," *Vacuum*, vol. 147, pp. 134-142, 2018
- [23] A.P. Bolshakov, V.G. Ralchenko, V.Y. Yurov, G. Shu, E.V. Bushuev, A.A. Khomich, E.E. Ashkinazi, D.N. Sovyk, I.A. Antonova, S.S. Savin, V.V. Voronov, M.Y. Shevchenko, B. Dai, J. Zhu, "Enhanced deposition rate of polycrystalline CVD diamond at high microwave power densities," *Diamond and Related Materials*, vol. 97, p. 107466, 2019
- [24] K. W. Hemawan, R. J. Hemley , "Optical emission diagnostics of plasmas in chemical vapor deposition of single-crystal diamond", *Journal of Vacuum Science & Technology A*, vol. 33, 2015
- [25] T. Teraji, T. Ito, "Homoepitaxial diamond growth by high-power microwave-plasma chemical vapor deposition," *Journal of Crystal Growth*, vol. 271, pp. 409-419, 2004
- [26] T. Sharda, M.M. Rahaman, Y. Nukaya, T. Soga, T. Jimbo, M. Umeno, "Structural and optical properties of diamond and nano-diamond films grown by microwave plasma chemical vapor deposition," *Diamond and Related Materials*, vol. 10, pp. 561-567, 2001
- [27] URL: <https://nandne.com/5-process-to-make-cvd-diamond-or-synthetic-diamond/>
- [28] T. Van Regemorter, "The influence of Dopants on the Growth of Diamond by CVD," *Digital Comprehensive Summaries of Uppsala Dissertations from the Faculty of Science and Technology*, vol. 594, p. 56, 2009
- [29] Z. Yiming, F. Larsson, and K. Larsson, "Effect of CVD diamond growth by doping with nitrogen," *Theoretical Chemistry Accounts*, vol. 133, p. 1432, 2014.

- [30] R. Ramamurti, M. Becker, T. Schuelke, T. Grotjohn, D. Reinhard, G. Swain, J. Asmussen, "Boron doped diamond deposited by microwave plasma-assisted CVD at low and high pressures," *Diamond and Related Materials*, vol. 17, pp. 481-485, 2008
- [31] V. Mortet, A. Taylor, Z. Vlčková Živcová, D. Machon, O. Frank, P. Hubík, D. Tremouilles, L. Kavan, "Analysis of heavily boron-doped diamond Raman spectrum," *Diamond and Related Materials*, vol. 88, pp. 163-166, 2018
- [32] X.H. Wang, G.-H.M. Ma, Wei Zhu, J.T. Glass, L. Bergman, K.F. Turner, R.J. Nemanich, "Effects of boron doping on the surface morphology and structural imperfections of diamond films," *Diamond and Related Materials*, vol. 1, pp. 828-835, 1992
- [33] Minghui Ding, Yanqing Liu, Xinru Lu, Yifeng Li, and Weizhong Tang, "Boron doped diamond films: A microwave attenuation material with high thermal conductivity," *Applied Physics Letters*, vol. 114, p. 162901, 2019
- [34] Polushin, Nikolay I., Alexander I. Laptev, Boris V. Spitsyn, Alexander E. Alexenko, Alexander M. Polyansky, Anatoly L. Maslov, and Tatiana V. Martynova, "Deposition of Boron-Doped Thin CVD Diamond Films from Methane-Triethyl Borate-Hydrogen Gas Mixture" *Processes*, vol. 8, p. 666, 2020
- [35] J. Xu, Y. Yokota, R. A. Wong, Y. Kim, and Y. Einaga, "Unusual Electrochemical Properties of Low-Doped Boron-Doped Diamond Electrodes Containing sp^2 Carbon," *Journal of the American Chemical Society*, vol. 142, pp. 2310-2316, 2020
- [36] T. A. Ivandini, T. Watanabe, T. Matsui, Y. Ootani, S. Iizuka, R. Toyoshima, H. Kodama, H. Kondoh, Y. Tateyama, Y. Einaga, "Influence of Surface Orientation on Electrochemical Properties of Boron-Doped Diamond," *The Journal of Physical Chemistry C*, vol. 123, pp. 5336-5344, 2019
- [37] Yao Y, Sang D, Duan S, Wang Q, Liu C, "Review on the Properties of Boron-Doped Diamond and One-Dimensional-Metal-Oxide Based P-N Heterojunction," *Molecules*, vol. 26, 2021
- [38] W. Chen, X. Lu, Q. Yang, C. Xiao, R. Sammynaiken, J. Maley, A. Hirose, "Effects of gas flow rate on diamond deposition in a microwave plasma reactor," *Thin Solid Films*, vol. 515, pp. 1970-1975, 2006
- [39] V Ralchenko, I Sychov, I Vlasov, A Vlasov, V Konov, A Khomich, S Voronina, "Quality of diamond wafers grown by microwave plasma CVD: effects of gas flow rate," *Diamond and Related Materials*, vol. 8, pp. 189-193, 1999
- [40] M. A. Chowdhury, D. M. Nuruzzaman, M. L. Rahaman, M. S. Islam, "The Effect of Gas Flow Rate on the Thin Film Deposition Rate on Carbon Steel Using Thermal CVD," *International Journal of Chemical Reactor Engineering*, vol. 9, 2011
- [41] F. G. Celii, D. White Jr., A. J. Purdes, "Effect of residence time on microwave plasma chemical vapor deposition of diamond," *Journal of Applied Physics*, vol. 70, pp. 5636-5646, 1991
- [42] J. Yu, R. Huang, L. Wen, C. Shi, "Nucleation kinetics of diamond in hot filament chemical vapour deposition," *Materials Research Bulletin*, vol. 34, pp. 2319-232, 1999

- [43] A. Croot, E.J.D. Mahoney, H. Dominguez-Andrade, M.N.R. Ashfold, N.A. Fox, "Diamond chemical vapor deposition using a zero-total gas flow environment," *Diamond and Related Materials*, vol. 109, p. 108011, 2020
- [44] A. Croot, "Boron and nitrogen in diamond: an ab initio simulation, plasma emission spectroscopy and material deposition & characterisation study," 2018
- [45] M.A. Elliott, P.W. May, J. Petherbridge, S.M. Leeds, M.N.R. Ashfold, W.N. Wang, "Optical emission spectroscopic studies of microwave enhanced diamond CVD using CH₄/CO₂ plasmas," *Diamond and Related Materials*, vol. 9, pp. 311-316, 2000
- [46] V.Yu. Yurov, E.V. Bushuev, A.P. Bolshakov, I.A. Antonova, V.G. Ralchenko, V.I. Konov, "Optical emission spectroscopy for diagnosis of diamond growth and etching processes in microwave plasma," *EPJ Web of Conferences*, vol. 149, 2017
- [47] A. Dychalska, P. Popielarski, W. Franków, K. Fabisiak, K. Paprocki, M. Szybowicz, "Study of CVD diamond layers with amorphous carbon admixture by Raman scattering spectroscopy," *Materials Science-Poland*, vol. 33, pp. 799-805, 2015
- [48] C.-s. Yan, Y. K. Vohra, H.-k. Mao, R. J. Hemley, "Very high growth rate chemical vapor deposition of single-crystal diamond," *Proceedings of the National Academy of Sciences*, vol. 99, pp. 12523-12525, 2002
- [49] URL:
<https://www.horiba.com/fileadmin/uploads/Scientific/Documents/Raman/Semiconductors01.pdf>
- [50] URL: <https://www.technoorg.hu/news-and-events/articles/high-resolution-scanning-electron-microscopy-1/>
- [51] S. Ohmagari, H. Yamada, H. Umezawa, A. Chayahara, T. Teraji, S.-i. Shikata, "Characterization of free-standing single-crystal diamond prepared by hot-filament chemical vapor deposition," *Diamond and Related Materials*, vol. 48, pp. 19-23, 2014
- [52] G. Friedlander, J. Kennedy, J. Miller, "Nuclear and Radiochemistry," John Wiley and Son, Inc., New York, 1966.
- [53] R. Gao, L. Liu, Y. Li, L. Shen, P. Wan, X. Ouyang, H. Zhang, J. Ruan, L. Zhou, L. Chen, X. Zhang, J. Liu, H. Li, M. Liu, X. Ouyang, "High-performance alpha-voltaic cell based on a 4H-SiC PIN junction diode," *Energy Conversion and Management*, vol. 252, p. 115090, 2022
- [54] V.S. Bormashov, S.Yu. Troschiev, S.A. Tarelkin, A.P. Volkov, D.V. Teteruk, A.V. Golovanov, M.S. Kuznetsov, N.V. Kornilov, S.A. Terentiev, V.D. Blank, "High power density nuclear battery prototype based on diamond Schottky diodes," *Diamond and Related Materials*, vol. 84, pp. 41-47, 2018
- [55] Rappaport, P., "The electron-voltaic effect in p-n junctions induced by betaparticle bombardment," *Phys. Rev.* 93, 246–247 (1954).
- [56] M.G. Spencer, T. Alam, "High power direct energy conversion by nuclear batteries," *Applied Physics Reviews*, vol. 6, p. 031305, 2019

[57] B. Liu, K. Liu, J. Zhao, W. Wang, V. Ralchenko, F. Geng, L. Yang, S. Zhang, J. Xue, J. Han, J. Zhu, B. Dai, "Enhanced performance of diamond Schottky nuclear batteries by using ZnO as electron transport layer," *Diamond and Related Materials*, vol. 109, p. 108026, 2020

[58] A.J. Eccles, T.A. Steele, A. Afzal, C.A. Rego, W. Ahmed, P.W. May, S.M. Leeds, "Influence of B- and N-doping levels on the quality and morphology of CVD diamond," *Thin Solid Films*, vol. 343-344, pp. 627-631, 1999

[59] F. Laugier, J.M. Hartmann, H. Moriceau, P. Holliger, R. Truche, J.C. Dupuy, "Backside and frontside depth profiling of B delta doping, at low energy, using new and previous magnetic SIMS instruments," *Applied Surface Science*, vol. 231-232, pp. 668-672, 2004